Macromolecules

Article

pubs.acs.org/Macromolecules

Dynamics of Shape-Persistent Giant Molecules: Zimm-like Melt, Elastic Plateau, and Cooperative Glass-like

GengXin Liu,[†] Xueyan Feng,[†] Kening Lang,[†] Ruimeng Zhang,[†] Dong Guo,[†] Shuguang Yang,[‡] and Stephen Z. D. Cheng*[,†]

[†]Department of Polymer Science, The University of Akron, Akron, Ohio 44325, United States

[‡]Center for Advanced Low-Dimension Materials, Donghua University, Shanghai 201620, China

Supporting Information

ABSTRACT: Giant molecules are a new class of soft matter having three-dimensional (3D) shapes and composed of chemically linked rigid molecular nanoparticles. Structurally, a 3D cluster of molecular nanoparticles can be one giant molecule or a few giant molecules associated together via specific interactions. The dynamics of clusters that are smaller than a critical diameter (~5 nm) presents a power law relaxation exponent of 0.7 at the high frequency region corresponding to segmental dynamics. Such scaling is similar to the result of the Zimm model although those clusters are neither chain-like nor in solution. Clusters that are larger than this critical diameter and formed by the association of giant molecules exhibit an elastic plateau due to caging of individual giant molecules. We hypothesize that clusters of such a large size cannot move as a whole, even above the glass transition temperature of the sample. They thus are "cooperative glass-like". A structural cluster of giant molecules could be abstracted as a dynamical cluster consisting of unlinked but cooperatively mobile beads. As derived in the random first-order transition theory, the cluster loses its mobility and reaches the glassy state when the diameter of the cluster is 6 times larger than the bead diameter. In our cases, we estimate that the critical diameter for these clusters is also approximately 6 times the bead diameter based on the glassy shear modulus of giant molecules. Thus, shape-persistent giant molecules may serve as a bridge between polymers and colloids and a platform to mimic cooperative rearrangements.

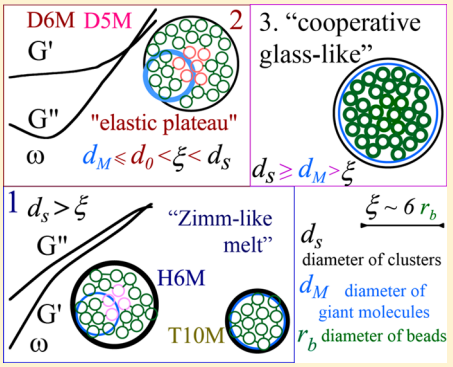

1. INTRODUCTION AND THEORETICAL BACKGROUND

Polymers are a class of one-dimensional (1D) macromolecules that traditionally have micrometer-scaled contour length. They are flexible and capable of curvilinear motion such as "reptation" above their glass transition temperatures (T_g).[1,2] The dynamics change dramatically for objects with 3D shapes.[3,4] Among them, dense colloidal suspensions are most studied. Their dynamics is governed by volume fractions and often described as jumping out of a cage.[5−8]

In the effort to study 3D macromolecules without solvent, several approaches have been made resulting in "soft particles". Multiarm star polymers and dendrimers also exhibit 3D shapes in the bulk.[9−21] However, they had no shape persistency because arms were 1D chains and may retract. Also, it was difficult to differentiate the effect of entanglement, the number of arms, and shape. Polymer grafted nanoparticles in the melt have been investigated,[22−33] in which they had a core of 10 nm or larger and squeezable long grafted chains as a shell. In these grafted nanoparticles, the core volume fractions were less than 20% of the overall volume. Their behavior was more associated with colloidal suspensions and governed by the volume fraction. Spherical assemblies of block copolymers have also been studied, but the volume fraction of the core was inevitably low.[34−37]

Single-chain aggregated nanoparticles or microgels were constructed by intrachain cross-linking an individual polystyrene chain to form a nanoparticle.[38,39] Their relaxation in the bulk was similar to the result of the Zimm model when their diameters were small. When their diameters became larger than a critical value of around 7 nm, an elastic plateau appeared.[38,39] However, this plateau modulus was reported to increase with increasing the diameter of the microgels, and the quantitative values were rather close to that of the entangled polystyrene.

Herein, we investigate the dynamics of recently developed giant molecules,[40−46] which have relatively persistent 3D shapes that range from 1 to 10 nm. It is expected that dynamic behaviors of 3D-shaped giant molecules in the bulk are different from those of 1D linear polymers. We ask in what diameter giant molecules would be too bulky to move in the bulk and act as colloidal particles on their own, if they are only stimulated by thermal energy k_BT (the system is not under large or destructive external deformation or force[24,47,48]).

With increasing diameter of giant molecules in 3D, we can imagine that their dynamics become slower or even immobile if they become too bulky in the bulk. These structural clusters

Received: May 19, 2017
Revised: August 7, 2017
Published: August 31, 2017

DOI: 10.1021/acs.macromol.7b01058
Macromolecules 2017, 50, 6637−6646

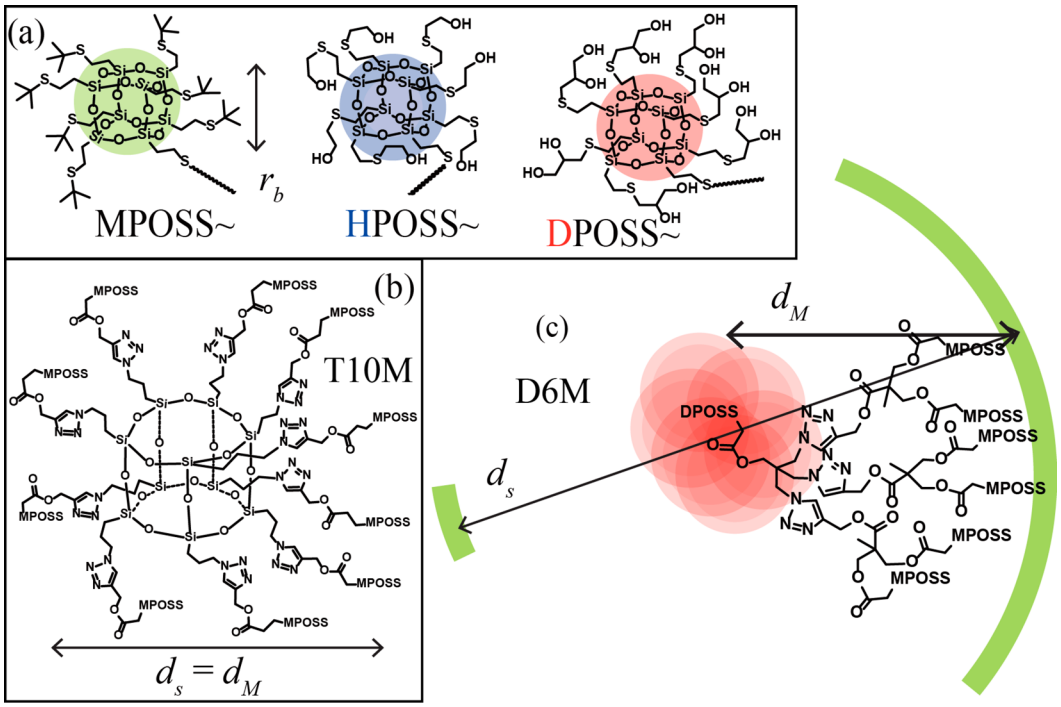

Figure 1. (a) Chemical structures of building blocks: MPOSS, HPOSS, and DPOSS. Chemical structures of linkers in (b) T10M and (c) D6M. The diameters are schematic. One T10M molecule acts as one structural cluster, while five D6M molecules associate together to form one structural cluster.

consist of chemically or physically linked hypothetical beads. We assume that such cluster is analogous to the dynamical cluster of cooperatively rearranging beads in glassy dynamics. Hence, a larger cluster could have slower dynamics, just as the dynamics slow down by forming larger cooperative rearranging clusters when it is approaching its glass transition.

In dynamics of general glasses, the critical cluster diameter or length scale of dynamic heterogeneities has been estimated based on extensive experimental results, for instance, 1 nm for glycerol[49] and 3 nm for *o*-terphenyl or poly(vinyl acetate).[50−54] In other words, within the 3D volume of this diameter or length scale, there were about 100 molecules in simple molecular systems[55,56] or segments in polymers.[57,58] A molecule in molecular systems or a few monomers in polymers was a hypothetical bead in glass-forming liquids.[57,58] The diameter of the bead r_b could be related to $V_{bead} = \pi r_b^3/6 = 24.9 k_B T_m/G$, with G as the shear modulus in the glassy state.[55] In general, the critical cluster diameter is about 6 times the diameter of the bead.[56,59−66]

When the temperature was decreasing toward its glass transition temperature (T_g), cooperative rearranging region grows in size and a growing number of beads start to move cooperatively as a cluster.[67] An answer to the dynamics slowdown was given by the random first-order transition theory,[55,68−70] one of the many theoretical treatments of glass transitions.[67,71−74] $\xi/r_b \propto [\ln(\tau/\tau_0)^{2/3}]$ was the relationship between τ, the relaxation time of the system, and ξ, the cluster diameter. When closing to the T_g, the critical cluster diameter was $\approx 6r_b$ (precisely, $5.8r_b$). Larger than this value, the cluster has no mobility.

We present the dynamics of four specifically chosen giant molecules with different cluster diameters out of a series of specially designed samples. Their building blocks are rigid molecular nanoparticles: polyhedral oligomeric silsesquioxane (POSS) cages. Their chemical structures and masses are precisely defined without polydispersity. These giant molecules in this study of dynamics only possess short-range orders in their structures. This is different from other giant molecules reported so far which can hierarchically self-assemble into superlattices, including spherical Frank−Kasper phases and quasicrystals.[40−44]

There are several ways to estimate and quantify the structural cluster and the mobile unit in these giant molecules. Structurally on one hand, the cluster diameter d_s can be deduced utilizing scattering techniques, such as X-ray (for nanometers) and light (for micrometers) scattering methods, depending on the cluster diameter and electron density of the cluster. A 3D cluster can be constituted of a single giant molecule or a few giant molecules associated together via specific interactions such as collective hydrogen bonding.[40−43]

On the other hand, the mobile unit diameter can be deduced from linear viscoelasticity measured by small-amplitude oscillatory shear (SAOS). It applies a small perturbation to the equilibrium sample and measures the elastic G' and viscous G'' responses corresponding to energy storage and dissipation. For a mobile unit driven by thermal energy k_BT with a mass M_0 and a diameter d_0, the characteristic modulus G_0 or elastic plateau modulus G_{pl} is inversely related to M_0 and d_0^3 as shown in eq 1:

$$G_0 \text{ or } G_{pl} \approx \frac{\rho RT}{M_0} = \frac{k_B T}{V} \approx \frac{6k_B T}{\pi d_0^3} \quad (1)$$

For unentangled polymers, G_0 depends on a polymer's molecular mass; for entangled polymers, G_{pl} depends on the entangled molecular mass; for dense colloidal suspensions, G_{pl} depends on caging correlated to their particle diameter;[5,75,76] for spherical assemblies of block copolymers, G_{pl} depends on their core diameter.[34−37,77]

DOI: 10.1021/acs.macromol.7b01058
Macromolecules 2017, 50, 6637−6646

Table 1. Summary of Parameters from Characterizations and Analysis[a]

	M_w [g/mol]	d_M [nm]	M_0 [g/mol]	no. of mol in the mobile unit	d_0 [nm]	d_s [nm]	no. of mol in the cluster	d_s/r_b	G_0, G_{pl} [Pa]	η_0 [Pa s]
T10M	15307	3.4	14400	0.94	3.4	3.3	0.91	3.9	2.10×10^5	2.9×10^6
H6M	9994	3.0	25600	2.6	4.1	4.5	3.4	5.2	1.18×10^5	2.4×10^6
D6M	10204	3.0	9660	0.95	2.9	5.2	5.3	6.1	3.13×10^5	2.0×10^7
D5M	9173	2.9	11400	1.24	3.1	7.3	16	8.5	2.64×10^5	N.A.

[a]Molecular mass M_w and diameter d_M of individual molecule, $M_w = \pi\rho d_M^3/6$; mass M_0 and diameter d_0 of the mobile unit; number of molecules in the mobile unit by $(d_0/d_M)^3$ or M_0/M_w; scattering correlation length or diameter of the cluster, d_s; number of molecules in the cluster by $(d_s/d_M)^3$; diameter of the cluster normalized by the diameter of the bead, d_s/r_b; characteristic modulus G_0 or elastic plateau modulus G_{pl} at 30 °C; zero-shear viscosity, η_0.

First, we address the correlations between the structural cluster obtained based on the scattering technique and the mobile unit determined by rheological measurements with respect to different cluster diameters. Second, differences in the dynamic behaviors of these giant molecules are categorized by the diameters of their 3D cluster. We seek general implications of dynamic behaviors of giant molecules correlated to the cluster diameters, in analogy to the control factor of molecular mass in polymers and volume fraction in colloidal suspensions. We further connect the structural cluster and mobile unit in giant molecular systems with the concept of cluster in glassy dynamics as put forward by the random first-order transition theory.

2. EXPERIMENTAL SECTION

The synthetic routes to construct these well-defined giant molecules have been established in a serial of studies.[40−45] Detailed syntheses are also given in the Supporting Information.

Rheological characterization was performed on a TA ARES-G2 using 8 mm parallel plates with a gap around 0.7 mm and with temperature control under a nitrogen atmosphere. Linear viscoelasticity measurements were taken typically under strain amplitude of 0.3%, which has been checked by performing a strain sweep from 10^{-3} to 10%. SAOS was carried out at angular frequency from 10^2 to 10^{-1} or 10^{-2} rad/s at one constant temperature.

Small-angle X-ray scattering (SAXS) experiments were performed at station 12-ID-B with X-ray energy of 14 keV at the Advanced Photon Source at the Argonne National Laboratory. The smoothed data were obtained by the LOWESS[78] method with a span of 0.01 or 0.02.

Diffuse reflectance infrared Fourier transform spectroscopy (DRIFTS)[79] was used to collect FT-IR spectra at different temperatures with a custom-built heating block. The heating block provided a stepwise increase of temperatures. Films of samples were prepared on an aluminum pan, which was then placed on top of the heating block and under a nitrogen atmosphere.

Differential scanning calorimetry (DSC) was performed on PerkinElmer DSC 8000 with intercooler II. The temperature is calibrated by indium also with 20 °C/min heating/cooling rate.

3. RESULTS AND DISCUSSION

3.1. Chemical Structures of Building Blocks and Samples. Three types of POSS cages are used as building blocks which are shown in Figure 1a. The hydrophobic POSS cages were functionalized with *tert*-butyl side groups and labeled as MPOSS. Bulky alkyl side groups prevent crystallization of MPOSS cages. The hydrophilic POSS cages were functionalized with 14 hydroxyl groups (labeled as DPOSS) or functionalized with 7 hydroxyl groups (labeled as HPOSS). DPOSS cages thus have a stronger association than HPOSS cages.[40−44]

The first giant molecule T10M contains 10 MPOSS cages chemically bonded to a core of T_{10}POSS via short linkers as shown in Figure 1b. In order to achieve larger structural cluster diameters, association by collective hydrogen bonding has been utilized to design the giant molecules. Both D6M and H6M possess six MPOSS cages connected to one DPOSS or one HPOSS cage, respectively, as shown in Figure 1c. The linkers in D6M and H6M are longer than that that in T10M. With an even longer linker, D5M possesses 5 MPOSS cages connected to one DPOSS cage as shown in Figure S1c.[46]

In the following study, we will show that the structural clusters are constructed by individual T10M or multiple molecules in the cases of D6M, H6M, and D5M via collective hydrogen bonding of hydrophilic POSS cages which form the cores of the clusters. The peripheries of the clusters are occupied by hydrophobic MPOSS cages. Therefore, for these four samples, van der Waals forces are the only interactions among the clusters.

3.2. Estimation of Characteristic Diameters of Building Block, Giant Molecules, and Structural Clusters. These giant molecules exhibit a similar T_g around 20 °C and similar densities around 1.20 g/cm^3. Combining this density and the molecular mass of one MPOSS cage (M_w, 1354.5 g/mol), the diameter of one MPOSS is thus estimated to be around 1.5 nm. If the individual giant molecule is assumed to be packed into a sphere with $M_w = \pi\rho d_M^3/6$, the diameters of giant molecule d_M would approximately be 3.4, 3.0, 3.0, and 2.9 nm for T10M, H6M, D6M, and D5M, respectively (Table 1).

Small-angle X-ray scattering (SAXS) patterns of these samples exhibit broad correlation scattering peaks as shown in Figure 2 (the raw data was given in Figure S3), indicating short-range ordered assembly structures. The weak second-order peak for D5M may be caused by residual order from the supramolecular spherical structure order (Figure S3).[46] The degree of this residual order is less than the liquid-like order

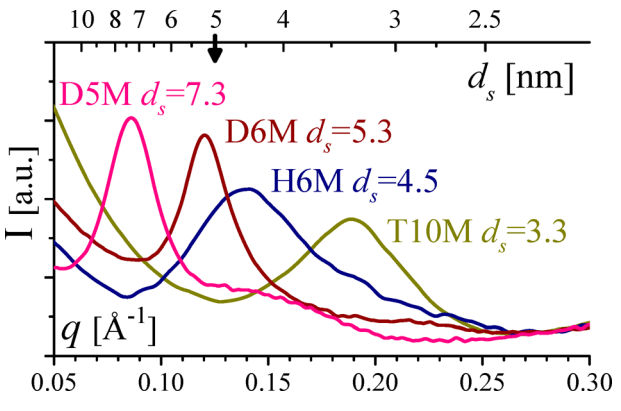

Figure 2. SAXS patterns all possess short-range orders and have correlation length d_s.

DOI: 10.1021/acs.macromol.7b01058
Macromolecules 2017, 50, 6637−6646

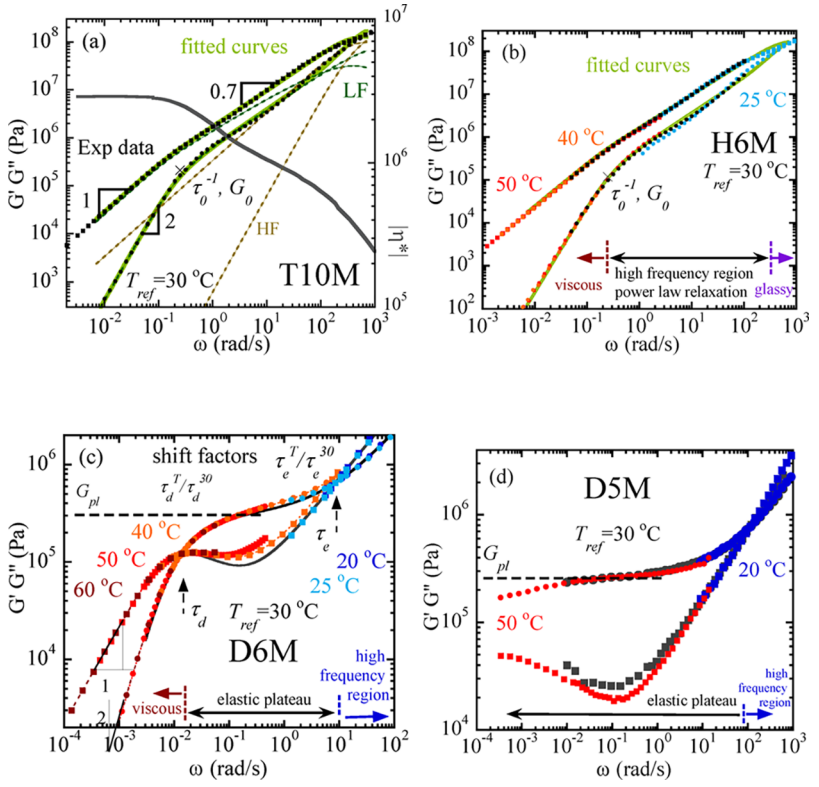

Figure 3. (a) SAOS master curves (G', ●; G'', ■) of T10M. Fitted curves in green show excellent match with experimental data. (b) SAOS master curves of H6M with different color presenting data obtained at different temperatures. Part of G' data show minor mismatch that do not fall onto the master curve. (c) SAOS of D6M at 30 °C are black lines. Measurements at lower temperatures are shifted to match the high frequency crossover at τ_e^{30}. Measurements at higher temperatures are shifted to match the terminal crossover at τ_d^{30}. Their shapes in elastic plateau region show mismatch. (d) SAOS of D5M at T_{ref} of 30 °C with data shifted from 20 and 50 °C. Elastic plateau spans more than 6 decades. τ_d is not accessible.

observed in the melts of star polymers[10,80,81] or spherical assemblies of diblock copolymers.[35,77,82] It does not significantly affect the dynamics and will be further illustrated in section 3.5.

The correlation length corresponding to the scattering peak, d_s, is assumed to be the average and characteristic structural cluster diameter, as if they are assumed to be spherical. Such estimations are crude but provide the essential guideline, even though these structural clusters are polydisperse and may not be perfect spheres.

For T10M and H6M to D6M and D5M, characteristic structural cluster diameters d_s increase from 3.3 and 4.5 nm to 5.2 and 7.3 nm, respectively (Table 1). Therefore, clusters with a diameter d_s contain $(d_s/d_M)^3$ molecules on average, equal to 1, 3, 5, and 16 for these samples, respectively. It suggests that individual T10M molecule acts as one structural cluster, while on average, three H6M, five D6M, and 16 D5M molecules associate together via collective hydrogen bonding to form clusters as illustrated in Figures 1b and 1c and Figure S1.

3.3. Small Structural Clusters of T10M and H6M Exhibit Scaling of 0.7 at High Frequencies as "Zimm-like Melts". Master curves of linear viscoelasticity constructed by time−temperature superposition and least-squares fitting are shown in Figure 3. Raw data are provided in Figure S4. The corresponding shift factors a_T and b_T are plotted in Figure 4 and Figure S4d.

Giant molecules T10M and H6M with small d_s values show liquid-like dynamics with $G' \propto \omega^{-2}$ and $G'' \propto \omega^{-1}$ at low frequencies. This dynamics corresponds to the viscous flow of the cluster as deduced in the next section. At high frequencies

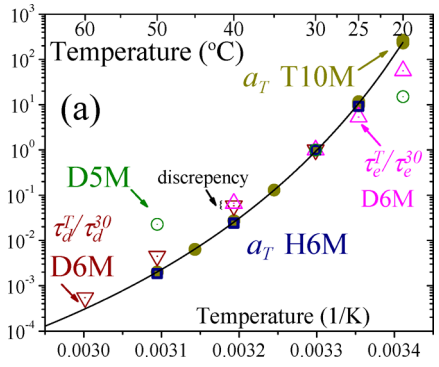

Figure 4. Shift factors a_T of T10M, H6M, and D5M, τ_d^T/τ_d^{30} and τ_e^T/τ_e^{30} of D6M. WLF fitting on T10M is the black curve.

for over 2 decades ($0.3 < \omega < 50$) before reaching the glassy state, G' and G'' are parallel and show a scaling exponent of 0.7. The dynamics in this high frequency region corresponds to segmental dynamics within the cluster. Such segments are referred to as beads.

A scaling exponent of 0.7 is also seen in solutions of polymers having high molecular masses, in some cases in melts of unentangled hyperbranched polymers and stars with multiple (>30) unentangled arms.[14−17] The scaling exponent in the result of the Zimm model can vary between 0.5 and 0.7 depending on the value of parameter h.[83] The Zimm model is a bead−spring model of linear chains that considered hydrodynamic interaction (quantified by h): the bead−bead correlation beyond close neighbor on the chain. The bead

DOI: 10.1021/acs.macromol.7b01058
Macromolecules 2017, 50, 6637−6646

here is a segment of Kuhn length.[57] The Rouse model is the simplest bead−spring model without considering hydrodynamic interaction.[84−88] It has identical G' and G'' and a scaling exponent of 0.5 in the high frequency region which has been observed on unentangled polymer melts.[85,86]

In the Rouse model, the relaxation modes approximate to $\tau_j = \tau_0/j^2$; j goes from 1 to N, the number of beads. In the Zimm model, $\tau_j = \tau_0/j^{2-h}$.[85,86] When $h = 0$, the Zimm model reduces to the Rouse model. In the θ solvent, h is 0.5 and the scaling exponent in the high frequency region correlates with the relaxation modes by $1/(2 - h) \approx 0.7$. When considering viscoelastic hydrodynamic interaction, a recent approach can also give $h > 0$.[89,90] An alternative mechanism other than hydrodynamics interaction also exists.[91−93] In various models of dendrimers solutions,[94−101] relaxation modes decay slower than j^2, $h > 0$, and scaling exponent larger than 0.5.

Giant molecules T10M and H6M are not linear chains in shape. We label their viscoelastic behavior as "Zimm-like melt" for the characteristic exponent of 0.7. In general, giant molecular clusters which are smaller than a certain diameter may all exhibit such viscoelastic behavior.

As shown in Figure 1, MPOSSs are densely linked together to a core. The molecular nanoparticle such as MPOSS with a diameter of 1.5 nm is rather large and shape-persistent and should not be treated as a point with negligible diameter. Thus, the movement of each MPOSS cage should influence other intracluster MPOSS cages within that mobile unit. A proper physical picture could be a cluster of beads, which would be analogous to the melt of dendrimers or solutions of chains. All three scenarios have stronger bead−bead correlations ($h > 0$) compared to the melt of linear chains where only two adjacent beads are correlated ($h = 0$).

We use h to quantify the strength of the bead−bead correlation, which alters the distribution of relaxation modes and influences scaling exponent in the high frequency region. Without formulating a detailed model, we numerically fit the experimental data by summation eq 2 of high frequency (HF, glassy dynamics,[102−104] eq 3) and low frequency (LF, the sum of Maxwell relaxation modes, eq 4) contributions. This helps to evaluate their dynamics quantitatively. There are total five variables in the fitting: h as an adjustment to relaxation modes, the characteristic modulus G_0 and relaxation time τ_0 for LF; and the shear modulus in the glassy state G_{HF} and when glassy response is reduced τ_{HF} for HF. The full range of dynamics is

$$G'_{total} = G'_{LF} + G'_{HF}; \quad G''_{total} = G''_{LF} + G''_{HF} \tag{2}$$

$$G^*_{HF} = G_{HF}\left(1 - \frac{1}{\sqrt{1 + i\omega\tau_{HF}}}\right) = G'_{HF} + iG''_{HF} \tag{3}$$

$$G'_{LF} = G_0 \sum_{j=1}^{N} \frac{\omega^2\tau_j^2}{1 + \omega^2\tau_j^2}; \quad G''_{LF} = G_0 \sum_{j=1}^{N} \frac{\omega\tau_j}{1 + \omega^2\tau_j^2} \tag{4}$$

A least-squares fit of these five parameters (G_{HF}, τ_{HF}, G_0, τ_0, h) on T10M leads to 2.75×10^8 Pa, 0.0025 s; 2.10×10^5 Pa, 4.02 s; and 0.63. Fitting on H6M leads to 3.60×10^8 Pa, 0.002 16 s; 1.18×10^5 Pa, 4.06 s; and 0.80. The fittings match well with the experimental results, and we indeed find large h values. If the value of h was constrained to zero as in the Rouse model, the fitting by only four parameters would not capture the shape of G' and G'' (Figure S5) even with glassy contributions.[105,106]

3.4. Small Structural Clusters of T10M and H6M Are Also Mobile Units. We then compare the M_0 and d_0 values of mobile units deduced from rheological measurements with the d_s value, the diameter of the structural cluster obtained based on the SAXS data, as well as the d_M value, the diameter of individual molecules. For T10M, an individual giant molecule acts not only as one structural cluster but also as the mobile unit stimulated by k_BT, namely, $d_s \approx d_0 \approx d_M \approx 3.4$ nm.

Since a lower G_0 value for H6M, its mobile unit thus possesses a larger mass and d_0 of 4.1 nm. The mobile unit has a diameter comparable to the structural cluster and is larger than individual T10M. In the mobile unit, number of molecules $(d_0/d_M)^3$ or M_0/M_w is 2.6. This means that stable dimers or trimers must be involved within the experimental temperature and frequency ranges, namely, $d_s \approx d_0 \approx 3d_M \approx 4.1$ nm.

The G' data obtained at 25 and 40 °C show slight deviations from the master curve, which would be caused by collective hydrogen bonding. Infrared spectroscopies (IR) in Figure 5 indicate that the broad absorption due to hydrogen-bonding shifts from 3400 to 3500 cm^{-1} with increasing temperature. Yet, there is no change at around 3650 cm^{-1}, revealing that the hydrogen bonding does not reach full dissociation.[107,108] The association to form dimers and trimers is thus stable under the present experimental conditions.

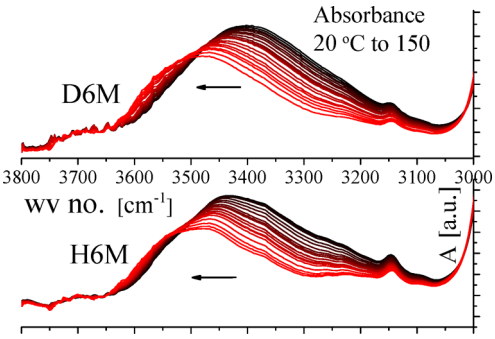

Figure 5. FT-IR spectrum of D6M and H6M at different temperatures show no sign of dissociated −OH around 3700 cm^{-1}.

Shifting factors a_T of T10M are not of the Arrhenius form (otherwise, it would be a straight line in Figure 4). A relationship of $\log a_T + 2.60 = -11.6[(T - 292.5)/(T - 292.5 + 36.4)]$ is obtained by fitting to Williams−Landel−Ferry equation and is plotted as a guide line.

3.5. Elastic Plateau on Large Structural Clusters of D6M and D5M. For D6M and D5M with d_s values larger than 5 nm, SAOS in Figures 3c,d reveals different viscoelastic behavior, namely, a distinct elastic plateau G_{pl}. Its value is determined by the value of G' at the same frequency where G'' shows the minimum.[109] D6M has one characteristic terminal relaxation, τ_d, at 73.5 s as the low frequency crossover. Segmental dynamics appear between τ_e and glassy region.

The elastic plateau of D5M spans more than 6 decades without reaching terminal relaxation at low frequency. This is more than 10^4 times slower than D6M, a drastic change considering that d_s increases by 30%. We cannot shift SAOS from even higher temperatures because this sample will form spherical ordered phases, quasi-crystal phase, and Frank−Kasper σ phase (~25 D5M assembled into a sphere)[46] when the temperature approaches 80 °C. In our experiments, D5M remains as disordered spherical assemblies without heating to high temperature.

DOI: 10.1021/acs.macromol.7b01058
Macromolecules 2017, 50, 6637−6646

The distinct elastic plateau G_{pl} is linked to the molecular mass of mobile unit M_0 by eq 1. As listed in Table 1, we find $M_0 \cong M_w$, which is the molecular mass of individual D6M or D5M molecule. It indicates that the mobile units in these two large clusters consists only individual molecules, namely, $d_0 \approx d_M \approx 3.0$ nm. This is thus clearly a different situation compared to small clusters of T10M and H6M, $d_0^{D5M} \approx d_0^{D6M} < d_0^{T10M} < d_0^{H6M}$, while $d_s^{D5M} > d_s^{D6M} > d_s^{H6M} > d_s^{T10M}$. There is a transition between d_s^{D6M} and d_s^{H6M}.

If G_{pl} was attributed to the mobility of entire clusters and proportional to $1/d_s^3$, we should see that G_{pl} decreases by a factor of 2.7 from D6M to D5M with increasing d_s. This is however not the case. If the cluster has mobility, the SAOS in Figure 3c should show another characteristic modulus around 6×10^4 Pa and another relaxation at lower frequency. Without such features, large clusters as a whole exhibit no sign of mobility, namely, $d_s > d_0$ for D6M to D5M.

3.6. Caging as the Origin of the Elastic Plateau. The existence of an elastic plateau also reveals a localized motion of individual molecules in the sample, reminiscent of tubes for polymers or caging for colloids. These giant molecules do not form networks or entanglement, and we have concluded that large clusters of D6M and D5M are immobile.[41,43−45] Thus, the reasonable origin of this elastic plateau is caging formed by immobile neighboring clusters.[5,6]

Such caging confines individual D6M or D5M to oscillate within the cage as illustrated in Figure 6. The transition from elastic plateau to viscous response at $\omega_d = \tau_d^{-1}$ corresponds to "breaking" of cages. Since clusters of D5M are larger than those of D6M, the cages are more effective and longer lasting, so τ_d is at a lower frequency than that of D6M.

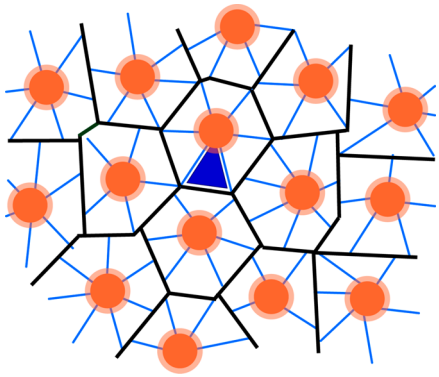

Figure 6. A scheme showing clusters of D6M formed by hydrophilic interaction among DPOSS. The hydrophilic core is marked in orange. The shell layer of the cluster is full of MPOSS which is hydrophobic. Black lines mark the boundary between clusters, while blue lines mark the boundary between individual molecules within one cluster.

From 30 to 60 °C, the diffusion coefficient of D6M $D_0 \approx k_BT/3\pi\eta d_M$ is estimated to increase from 10^{-20} to 10^{-17} m^2/s. It is still impractical to measure. The time needed for individual D6M to diffuse by a distance d_M of 3 nm would be $\tau_D = d_M^2/D \approx 18\tau_d \approx 10^3$ s at 30 °C. A similar trend of diffusion time τ_D longer than the terminal relaxation τ_d has been observed on associative polymers.[110]

The terminal relaxation or "breaking" of cages may arise from a transient dissociation of hydrogen bonding. However, reassociation could happen instantly since there is no dissociated hydroxyl group as revealed by the IR spectrum in Figure 5. Hydrogen bonding can hold the clusters in our experimental temperature range, although failure of time−temperature superposition is evidenced by the mismatch of G' and G'' in Figure 3c,d. The discrepancy in temperature dependence between hydrogen bonding and other van der Waals interactions is evidenced by the mismatch between shift factors τ_d^{40}/τ_d^{30} (≈0.058) and τ_e^{40}/τ_e^{30} (≈0.066) in Figure 4. In our system, this discrepancy value is estimated to be 14% and almost undistinguishable in logarithm scale. The dynamics of D6M and D5M is caging on individual molecules, different from the liquid-like viscous response of T10M and H6M. This might be the reason they have different shifting factors a_T in Figure 4.

3.7. Critical Diameter of the 3D Structural Cluster and "Cooperative Glass-like". Prior results and discussions show that the structural cluster is the mobile unit as long as the structural cluster is smaller than a critical diameter. When the structural cluster is larger than the critical value, the mobile unit, however, cannot exceed this value.

We suggest that the structural cluster of D6M or D5M is larger than a critical diameter of ∼5 nm. Larger than this critical diameter, clusters behave like particles with no mobility if only stimulated by k_BT. The immobile clusters cause effective caging which then causes elastic plateau and different viscoelasticity from those small clusters of H6M or T10M. This critical diameter thus marks a transition from liquid-like viscous to glass-like elastic behavior. It is analogous to the critical volume fraction for colloidal suspensions when becoming glassy and the critical molecular mass for polymers when becoming entangled.

In the present system of giant molecules, the diameter of bead r_b is ≈0.86 nm as determined by $G \approx 4 \times 10^8$ Pa. This glassy modulus has similar value across samples, which is G_{HF} from fitting of H6M and T10M. It can also be read from Figures S4 and S7. This r_b is a reasonable value which is smaller than the diameter of MPOSS cage. It means bulky alkyl side groups together with the POSS core act as more than one basic unit (bead) in glassy dynamics. Hence, the critical diameter of clusters ξ according to random first transition theory is ≈5.0 nm, in agreement with the experimental boundary found as between the diameters of structural clusters of H6M and D6M.

"Cooperative glass-like" behavior would be achieved when diameters of giant molecules are larger than ξ (when there are about a hundred beads in the cluster) so that it is impossible to move them by overcoming the entropic barrier of pushing their neighbors away. This would be a unique state of 3D giant molecules. In comparison, polymers always have unrestricted 1D motion above T_g, no matter how long the chains are.[111,112]

If one D6M molecule gets out of the cluster of D6M, the remaining cluster may be below the critical diameter. If one D5M molecule gets out of the cluster of D5M, the remaining cluster is still above the critical diameter. This may explain the slowdown more than 10^4 times from D6M to D5M.

The T_g of the system would be influenced by (1) the interaction among molecular nanoparticles and (2) the connectivity of molecular nanoparticles within giant molecules or clusters. When the connectivity remains the same but the interaction increases (by changing the pendant groups from *tert*-butyl $-C(CH_3)_3$ groups to more interactive groups such as phenyl groups or hydrogen bonding), the T_g value could increase. In future, we will verify if the critical diameter $\approx 6r_b$ is universal on describing the dynamics of giant molecules, when the experimental temperature is above their T_g values.

DOI: 10.1021/acs.macromol.7b01058
Macromolecules 2017, 50, 6637−6646

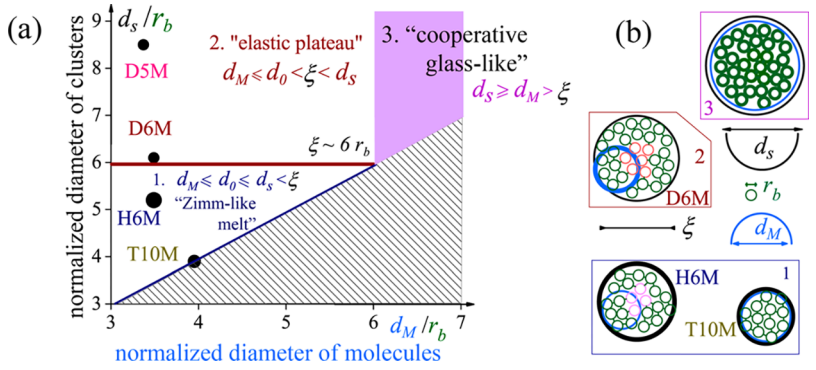

Figure 7. (a) Illustrations of three types of dynamics of giant molecules in a plot of the diameter of cluster d_s versus the diameter of individual molecule d_M, both normalized by the diameter of the bead r_b. Black filled circles mark the four samples studied here (size of the symbol is proportional to d_0, the diameter of the mobile unit). The critical diameter ξ for cooperative rearrangements is $6r_b$. The line-shaded region in the lower right is not realistic, as d_s deduced from SAXS cannot be smaller than d_M. (b) Illustrations of four clusters of beads belonging to three types of dynamics with the critical diameter ξ as a marker. The green circle represents a bead; pink circles represent the hydrophilic domain in H6M and D6M. The blue circle represents a giant molecule; the black circle represents the cluster. The thicker circle is the mobile unit of that sample.

4. CONCLUSION

In summary, as shown in Figure 7, we identify three types of dynamic behavior of shape-persistent giant molecules.

The 3D structural cluster is determined by the scattering technique, which is consisted of one giant molecule or a few giant molecules associated together via specific interactions. The mobile unit is determined by rheological measurements. In glassy dynamics, the concept of cluster is used to describe the length scale of dynamics heterogeneities as clusters of cooperatively rearranging beads, with bead represents segment and the basic unit in glass-forming liquids.

(1) If the diameter of the 3D cluster d_s is smaller than the critical diameter $\approx 6r_b$, its linear viscoelasticity shows scaling exponent of 0.7 at high frequencies, similar to the result of the Zimm model, suggesting a strong bead−bead correlation. This is the case of T10M and H6M.

(2) Clusters in the cases of D6M and D5M that possess a d_s larger than $6r_b$ show an elastic plateau modulus G_{pl} corresponding to caging on individual molecule. Note that the clusters here are consisted of multiple molecules via collective hydrogen bonding. Dissociation/association of hydrogen bonding at the terminal relaxation marks the end of the elastic plateau and caging.

(3) We suggest that if the diameter of giant molecules d_M is larger than the critical diameter, such giant molecules would be immobile under thermal energy k_BT even above the T_g of the sample and become "cooperative glass-like". This new type of dynamics is marked as $d_s \geq d_s$ and $d_M > \xi$. It is a unique feature of 3D giant molecules.

The critical diameter for immobile clusters is evidenced by the presence of an elastic plateau caused by effective caging of individual molecules and the lack of a characteristic modulus and relaxation corresponding to the entire cluster. This critical diameter is in agreement with the limit of cooperative rearrangements ξ in experiments and in the random first-order transition theory.

It is thus anticipated that shape-persistent giant molecules not only demonstrate diverse dynamics as a new class of soft matter but also can serve as a new bridge between polymers and colloids[19] and a new platform to mimic cooperative rearrangements and dynamic heterogeneities.

■ ASSOCIATED CONTENT

Supporting Information

The Supporting Information is available free of charge on the ACS Publications website at DOI: 10.1021/acs.macromol.7b01058.

Figures S1−S14; experimental details (PDF)

■ AUTHOR INFORMATION

Corresponding Author

*E-mail: scheng@uakron.edu (S.Z.D.C.).

ORCID

GengXin Liu: 0000-0002-2998-8572

Stephen Z. D. Cheng: 0000-0003-1448-0546

Notes

The authors declare no competing financial interest.

■ ACKNOWLEDGMENTS

This work is supported by NSF DMR-1408872. The authors acknowledge the help from Hailiang Jin and Prof. Steven S. C. Chuang for IR measurements. The authors also acknowledge the help from Dr. Tao Li and the use of Advanced Photon Source, an Office of Science User Facility operated for the U.S. Department of Energy by Argonne National Laboratory.

■ REFERENCES

(1) de Gennes, P. G. Reptation of a Polymer Chain in the Presence of Fixed Obstacles. *J. Chem. Phys.* **1971**, *55*, 572−579.

(2) Rubinstein, M.; Colby, R. H. *Polymer Physics*; Oxford University Press: New York, 2003; p 440.

(3) Mewis, J.; Wagner, N. J. *Colloidal Suspension Rheology*; Cambridge University Press: 2012.

(4) Silvera Batista, C. A.; Larson, R. G.; Kotov, N. A. Nonadditivity of nanoparticle interactions. *Science* **2015**, *350*, 1242477.

(5) Mason, T. G.; Weitz, D. A. Linear Viscoelasticity of Colloidal Hard Sphere Suspensions near the Glass Transition. *Phys. Rev. Lett.* **1995**, *75*, 2770−2773.

(6) Weeks, E. R.; Crocker, J. C.; Levitt, A. C.; Schofield, A.; Weitz, D. A. Three-Dimensional Direct Imaging of Structural Relaxation Near the Colloidal Glass Transition. *Science* **2000**, *287*, 627−631.

(7) Schweizer, K. S. Relationships between the single particle barrier hopping theory and thermodynamic, disordered media, elastic, and jamming models of glassy systems. *J. Chem. Phys.* **2007**, *127*, 164506.

DOI: 10.1021/acs.macromol.7b01058
Macromolecules 2017, 50, 6637−6646

(8) Mattsson, J.; Wyss, H. M.; Fernandez-Nieves, A.; Miyazaki, K.; Hu, Z.; Reichman, D. R.; Weitz, D. A. Soft colloids make strong glasses. *Nature* **2009**, *462*, 83−86.
(9) Roovers, J. Viscoelastic properties of 32-arm star polybutadienes. *Macromolecules* **1991**, *24*, 5895−5896.
(10) Pakula, T.; Vlassopoulos, D.; Fytas, G.; Roovers, J. Structure and Dynamics of Melts of Multiarm Polymer Stars. *Macromolecules* **1998**, *31*, 8931−8940.
(11) Uppuluri, S.; Morrison, F. A.; Dvornic, P. R. Rheology of Dendrimers. 2. Bulk Polyamidoamine Dendrimers under Steady Shear, Creep, and Dynamic Oscillatory Shear. *Macromolecules* **2000**, *33*, 2551−2560.
(12) Vlassopoulos, D.; Fytas, G.; Pakula, T.; Roovers, J. Multiarm star polymers dynamics. *J. Phys.: Condens. Matter* **2001**, *13*, R855.
(13) Tande, B. M.; Wagner, N. J.; Kim, Y. H. Influence of End Groups on Dendrimer Rheology and Conformation. *Macromolecules* **2003**, *36*, 4619−4623.
(14) Dorgan, J. R.; Knauss, D. M.; Al-Muallem, H. A.; Huang, T.; Vlassopoulos, D. Melt Rheology of Dendritically Branched Polystyrenes. *Macromolecules* **2003**, *36*, 380−388.
(15) Kwak, S.-Y.; Choi, J.; Song, H. J. Viscoelastic Relaxation and Molecular Mobility of Hyperbranched Poly(ε-caprolactone)s in Their Melt State. *Chem. Mater.* **2005**, *17*, 1148−1156.
(16) Kainthan, R. K.; Muliawan, E. B.; Hatzikiriakos, S. G.; Brooks, D. E. Synthesis, Characterization, and Viscoelastic Properties of High Molecular Weight Hyperbranched Polyglycerols. *Macromolecules* **2006**, *39*, 7708−7717.
(17) Ruymbeke, E. v.; Muliawan, E. B.; Vlassopoulos, D.; Gao, H.; Matyjaszewski, K. Melt rheology of star polymers with large number of small arms, prepared by crosslinking poly(n-butyl acrylate) macromonomers via ATRP. *Eur. Polym. J.* **2011**, *47*, 746−751.
(18) Snijkers, F.; Cho, H. Y.; Nese, A.; Matyjaszewski, K.; Pyckhout-Hintzen, W.; Vlassopoulos, D. Effects of Core Microstructure on Structure and Dynamics of Star Polymer Melts: From Polymeric to Colloidal Response. *Macromolecules* **2014**, *47*, 5347−5356.
(19) Seghrouchni, R.; Petekidis, G.; Vlassopoulos, D.; Fytas, G.; Semenov, A.; Roovers, J.; Fleischer, G. Controlling the dynamics of soft spheres: From polymeric to colloidal behavior. *EPL (Europhysics Letters)* **1998**, *42*, 271.
(20) Johnson, K. J.; Glynos, E.; Sakellariou, G.; Green, P. Dynamics of Star-Shaped Polystyrene Molecules: From Arm Retraction to Cooperativity. *Macromolecules* **2016**, *49*, 5669−5676.
(21) Pakula, T.; Geyler, S.; Edling, T.; Boese, D. Relaxation and viscoelastic properties of complex polymer systems. *Rheol. Acta* **1996**, *35*, 631−644.
(22) Yu, H.-Y.; Koch, D. L. Structure of Solvent-Free Nanoparticle−Organic Hybrid Materials. *Langmuir* **2010**, *26*, 16801−16811.
(23) Agarwal, P.; Qi, H.; Archer, L. A. The Ages in a Self-Suspended Nanoparticle Liquid. *Nano Lett.* **2010**, *10*, 111−115.
(24) Agarwal, P.; Archer, L. A. Strain-accelerated dynamics of soft colloidal glasses. *Phys. Rev. E* **2011**, *83*, 041402.
(25) Wen, Y. H.; Schaefer, J. L.; Archer, L. A. Dynamics and Rheology of Soft Colloidal Glasses. *ACS Macro Lett.* **2015**, *4*, 119−123.
(26) Srivastava, S.; Agarwal, P.; Mangal, R.; Koch, D. L.; Narayanan, S.; Archer, L. A. Hyperdiffusive Dynamics in Newtonian Nanoparticle Fluids. *ACS Macro Lett.* **2015**, *4*, 1149−1153.
(27) Agrawal, A.; Yu, H.-Y.; Sagar, A.; Choudhury, S.; Archer, L. A. Molecular Origins of Temperature-Induced Jamming in Self-Suspended Hairy Nanoparticles. *Macromolecules* **2016**, *49*, 8738−8747.
(28) Goel, V.; Pietrasik, J.; Dong, H.; Sharma, J.; Matyjaszewski, K.; Krishnamoorti, R. Structure of Polymer Tethered Highly Grafted Nanoparticles. *Macromolecules* **2011**, *44*, 8129−8135.
(29) Zhao, D.; Ge, S.; Senses, E.; Akcora, P.; Jestin, J.; Kumar, S. K. Role of Filler Shape and Connectivity on the Viscoelastic Behavior in Polymer Nanocomposites. *Macromolecules* **2015**, *48*, 5433−5438.
(30) Moll, J. F.; Akcora, P.; Rungta, A.; Gong, S.; Colby, R. H.; Benicewicz, B. C.; Kumar, S. K. Mechanical Reinforcement in Polymer Melts Filled with Polymer Grafted Nanoparticles. *Macromolecules* **2011**, *44*, 7473−7477.
(31) Baeza, G. P.; Dessi, C.; Costanzo, S.; Zhao, D.; Gong, S.; Alegria, A.; Colby, R. H.; Rubinstein, M.; Vlassopoulos, D.; Kumar, S. K. Network dynamics in nanofilled polymers. *Nat. Commun.* **2016**, *7*, 11368.
(32) Green, P. F.; Oh, H.; Akcora, P.; Kumar, S. K. Structure and Dynamics of Polymer Nanocomposites Involving Chain-Grafted Spherical Nanoparticles. In *Dynamics of Soft Matter: Neutron Applications*; García Sakai, V., Alba-Simionesco, C., Chen, S.-H., Eds.; Springer: Boston, MA, 2012; pp 349−366.
(33) Kumar, S. K.; Jouault, N.; Benicewicz, B.; Neely, T. Nanocomposites with Polymer Grafted Nanoparticles. *Macromolecules* **2013**, *46*, 3199−3214.
(34) Sebastian, J. M.; Graessley, W. W.; Register, R. A. Steady-shear rheology of block copolymer melts and concentrated solutions: Defect-mediated flow at low stresses in body-centered-cubic systems. *J. Rheol.* **2002**, *46*, 863−879.
(35) Sebastian, J. M.; Lai, C.; Graessley, W. W.; Register, R. A. Steady-Shear Rheology of Block Copolymer Melts and Concentrated Solutions: Disordering Stress in Body-Centered-Cubic Systems. *Macromolecules* **2002**, *35*, 2707−2713.
(36) Adams, J. L.; Graessley, W. W.; Register, R. A. Rheology and the Microphase Separation Transition in Styrene-Isoprene Block Copolymers. *Macromolecules* **1994**, *27*, 6026−6032.
(37) Kossuth, M. B.; Morse, D. C.; Bates, F. S. Viscoelastic behavior of cubic phases in block copolymer melts. *J. Rheol.* **1999**, *43*, 167−196.
(38) Antonietti, M.; Pakula, T.; Bremser, W. Rheology of Small Spherical Polystyrene Microgels: A Direct Proof for a New Transport Mechanism in Bulk Polymers besides Reptation. *Macromolecules* **1995**, *28*, 4227−4233.
(39) Tuteja, A.; Mackay, M. E.; Hawker, C. J.; Van Horn, B.; Ho, D. L. Molecular architecture and rheological characterization of novel intramolecularly crosslinked polystyrene nanoparticles. *J. Polym. Sci., Part B: Polym. Phys.* **2006**, *44*, 1930−1947.
(40) Yu, X.; Yue, K.; Hsieh, I.-F.; Li, Y.; Dong, X.-H.; Liu, C.; Xin, Y.; Wang, H.-F.; Shi, A.-C.; Newkome, G. R.; Ho, R.-M.; Chen, E.-Q.; Zhang, W.-B.; Cheng, S. Z. D. Giant surfactants provide a versatile platform for sub-10-nm nanostructure engineering. *Proc. Natl. Acad. Sci. U. S. A.* **2013**, *110*, 10078−10083.
(41) Zhang, W. B.; Yu, X.; Wang, C. L.; Sun, H. J.; Hsieh, I. F.; Li, Y.; Dong, X. H.; Yue, K.; Van Horn, R.; Cheng, S. Z. D. Molecular Nanoparticles Are Unique Elements for Macromolecular Science: From "Nanoatoms" to Giant Molecules. *Macromolecules* **2014**, *47*, 1221−1239.
(42) Feng, X.; Zhu, S.; Yue, K.; Su, H.; Guo, K.; Wesdemiotis, C.; Zhang, W.-B.; Cheng, S. Z. D.; Li, Y. T10 Polyhedral Oligomeric Silsesquioxane-Based Shape Amphiphiles with Diverse Head Functionalities via "Click" Chemistry. *ACS Macro Lett.* **2014**, *3*, 900−905.
(43) Huang, M.; Hsu, C.-H.; Wang, J.; Mei, S.; Dong, X.; Li, Y.; Li, M.; Liu, H.; Zhang, W.; Aida, T.; Zhang, W.-B.; Yue, K.; Cheng, S. Z. D. Selective assemblies of giant tetrahedra via precisely controlled positional interactions. *Science* **2015**, *348*, 424−428.
(44) Yue, K.; Huang, M.; Marson, R. L.; He, J.; Huang, J.; Zhou, Z.; Wang, J.; Liu, C.; Yan, X.; Wu, K.; Guo, Z.; Liu, H.; Zhang, W.; Ni, P.; Wesdemiotis, C.; Zhang, W.-B.; Glotzer, S. C.; Cheng, S. Z. D. Geometry induced sequence of nanoscale Frank−Kasper and quasicrystal mesophases in giant surfactants. *Proc. Natl. Acad. Sci. U. S. A.* **2016**, *113*, 14195−14200.
(45) Feng, X.; Zhang, R.; Li, Y.; Hong, Y.-l.; Guo, D.; Lang, K.; Wu, K.-Y.; Huang, M.; Mao, J.; Wesdemiotis, C.; Nishiyama, Y.; Zhang, W.; Zhang, W.; Miyoshi, T.; Li, T.; Cheng, S. Z. D. Hierarchical Self-Organization of ABn Dendron-like Molecules into Supramolecular Lattice Sequence. *ACS Cent. Sci.* **2017**, *3*, 860−867.
(46) Feng, X.; et al. Manuscript in preparation.
(47) Sollich, P.; Lequeux, F.; Hébraud, P.; Cates, M. E. Rheology of Soft Glassy Materials. *Phys. Rev. Lett.* **1997**, *78*, 2020−2023.
(48) Wyss, H. M.; Miyazaki, K.; Mattsson, J.; Hu, Z.; Reichman, D. R.; Weitz, D. A. Strain-Rate Frequency Superposition: A Rheological

DOI: 10.1021/acs.macromol.7b01058
Macromolecules 2017, 50, 6637−6646

Probe of Structural Relaxation in Soft Materials. *Phys. Rev. Lett.* **2007**, *98*, 238303.
(49) Reinsberg, S. A.; Qiu, X. H.; Wilhelm, M.; Spiess, H. W.; Ediger, M. D. Length scale of dynamic heterogeneity in supercooled glycerol near Tg. *J. Chem. Phys.* **2001**, *114*, 7299−7302.
(50) Cicerone, M. T.; Blackburn, F. R.; Ediger, M. D. How do molecules move near Tg? Molecular rotation of six probes in o-terphenyl across 14 decades in time. *J. Chem. Phys.* **1995**, *102*, 471−479.
(51) Cicerone, M. T.; Ediger, M. D. Relaxation of spatially heterogeneous dynamic domains in supercooled ortho-terphenyl. *J. Chem. Phys.* **1995**, *103*, 5684−5692.
(52) Tracht, U.; Wilhelm, M.; Heuer, A.; Feng, H.; Schmidt-Rohr, K.; Spiess, H. W. Length Scale of Dynamic Heterogeneities at the Glass Transition Determined by Multidimensional Nuclear Magnetic Resonance. *Phys. Rev. Lett.* **1998**, *81*, 2727−2730.
(53) Reinsberg, S. A.; Heuer, A.; Doliwa, B.; Zimmermann, H.; Spiess, H. W. Comparative study of the NMR length scale of dynamic heterogeneities of three different glass formers. *J. Non-Cryst. Solids* **2002**, *307−310*, 208−214.
(54) Vidal Russell, E.; Israeloff, N. E. Direct observation of molecular cooperativity near the glass transition. *Nature* **2000**, *408*, 695−698.
(55) Wisitsorasak, A.; Wolynes, P. G. On the strength of glasses. *Proc. Natl. Acad. Sci. U. S. A.* **2012**, *109*, 16068−16072.
(56) Berthier, L.; Biroli, G.; Bouchaud, J.-P.; Cipelletti, L.; Masri, D. E.; L'Hôte, D.; Ladieu, F.; Pierno, M. Direct Experimental Evidence of a Growing Length Scale Accompanying the Glass Transition. *Science* **2005**, *310*, 1797−1800.
(57) Ding, Y.; Sokolov, A. P. Comment on the dynamic bead size and Kuhn segment length in polymers: Example of polystyrene. *J. Polym. Sci., Part B: Polym. Phys.* **2004**, *42*, 3505−3511.
(58) Agapov, A.; Sokolov, A. P. Size of the Dynamic Bead in Polymers. *Macromolecules* **2010**, *43*, 9126−9130.
(59) Donati, C.; Franz, S.; Glotzer, S. C.; Parisi, G. Theory of non-linear susceptibility and correlation length in glasses and liquids. *J. Non-Cryst. Solids* **2002**, *307-310*, 215−224.
(60) Ediger, M. D. Length Scale of Dynamic Heterogeneity in Supercooled d-Sorbitol: Comparison to Model Predictions. *J. Phys. Chem. B* **2003**, *107*, 459−464.
(61) Arndt, M.; Stannarius, R.; Groothues, H.; Hempel, E.; Kremer, F. Length Scale of Cooperativity in the Dynamic Glass Transition. *Phys. Rev. Lett.* **1997**, *79*, 2077−2080.
(62) Ediger, M. D. Spatially Heterogeneous Dynamics in Supercooled Liquids SPATIALLY HETEROGENEOUS DYNAMICS IN SUPERCOOLED LIQUIDS. *Annu. Rev. Phys. Chem.* **2000**, *51*, 99−128.
(63) Donth, E. The size of cooperatively rearranging regions at the glass transition. *J. Non-Cryst. Solids* **1982**, *53*, 325−330.
(64) Ediger, M. D.; Angell, C. A.; Nagel, S. R. Supercooled Liquids and Glasses. *J. Phys. Chem.* **1996**, *100*, 13200−13212.
(65) Glotzer, S. C. Spatially heterogeneous dynamics in liquids: insights from simulation. *J. Non-Cryst. Solids* **2000**, *274*, 342−355.
(66) Dalle-Ferrier, C.; Thibierge, C.; Alba-Simionesco, C.; Berthier, L.; Biroli, G.; Bouchaud, J. P.; Ladieu, F.; L'Hôte, D.; Tarjus, G. Spatial correlations in the dynamics of glassforming liquids: Experimental determination of their temperature dependence. *Phys. Rev. E* **2007**, *76*, 041510.
(67) Adam, G.; Gibbs, J. H. On the Temperature Dependence of Cooperative Relaxation Properties in Glass-Forming Liquids. *J. Chem. Phys.* **1965**, *43*, 139−146.
(68) Xia, X.; Wolynes, P. G. Fragilities of liquids predicted from the random first order transition theory of glasses. *Proc. Natl. Acad. Sci. U. S. A.* **2000**, *97*, 2990−2994.
(69) Xia, X.; Wolynes, P. G. Microscopic Theory of Heterogeneity and Nonexponential Relaxations in Supercooled Liquids. *Phys. Rev. Lett.* **2001**, *86*, 5526−5529.
(70) Lubchenko, V.; Wolynes, P. G. Barrier softening near the onset of nonactivated transport in supercooled liquids: Implications for establishing detailed connection between thermodynamic and kinetic anomalies in supercooled liquids. *J. Chem. Phys.* **2003**, *119*, 9088−9105.
(71) Turnbull, D.; Cohen, M. H. Free-Volume Model of the Amorphous Phase: Glass Transition. *J. Chem. Phys.* **1961**, *34*, 120−125.
(72) Turnbull, D.; Cohen, M. H. On the Free-Volume Model of the Liquid-Glass Transition. *J. Chem. Phys.* **1970**, *52*, 3038−3041.
(73) Gotze, W.; Sjogren, L. Relaxation processes in supercooled liquids. *Rep. Prog. Phys.* **1992**, *55*, 241.
(74) Reichman, D. R.; Charbonneau, P. Mode-coupling theory. *J. Stat. Mech.: Theory Exp.* **2005**, *2005*, P05013.
(75) Shikata, T.; Pearson, D. S. Viscoelastic behavior of concentrated spherical suspensions. *J. Rheol.* **1994**, *38*, 601−616.
(76) Koumakis, N.; Pamvouxoglou, A.; Poulos, A. S.; Petekidis, G. Direct comparison of the rheology of model hard and soft particle glasses. *Soft Matter* **2012**, *8*, 4271−4284.
(77) Lee, S.; Leighton, C.; Bates, F. S. Sphericity and symmetry breaking in the formation of Frank−Kasper phases from one component materials. *Proc. Natl. Acad. Sci. U. S. A.* **2014**, *111*, 17723−17731.
(78) Cleveland, W. S.; Devlin, S. J. Locally Weighted Regression: An Approach to Regression Analysis by Local Fitting. *J. Am. Stat. Assoc.* **1988**, *83*, 596−610.
(79) Yu, J.; Chuang, S. S. C. The Structure of Adsorbed Species on Immobilized Amines in CO_2 Capture: An in Situ IR Study. *Energy Fuels* **2016**, *30*, 7579−7587.
(80) Vlassopoulos, D.; Pakula, T.; Fytas, G.; Roovers, J.; Karatasos, K.; Hadjichristidis, N. Ordering and viscoelastic relaxation in multiarm star polymer melts. *EPL (Europhysics Letters)* **1997**, *39*, 617.
(81) Vlassopoulos, D.; Pakula, T.; Fytas, G.; Pitsikalis, M.; Hadjichristidis, N. Controlling the self-assembly and dynamic response of star polymers by selective telechelic functionalization. *J. Chem. Phys.* **1999**, *111*, 1760−1764.
(82) Kim, K.; Schulze, M. W.; Arora, A.; Lewis, R. M.; Hillmyer, M. A.; Dorfman, K. D.; Bates, F. S. Thermal processing of diblock copolymer melts mimics metallurgy. *Science* **2017**, *356*, 520−523.
(83) Zimm, B. H. Dynamics of Polymer Molecules in Dilute Solution: Viscoelasticity, Flow Birefringence and Dielectric Loss. *J. Chem. Phys.* **1956**, *24*, 269−278.
(84) Rouse, P. E. A Theory of the Linear Viscoelastic Properties of Dilute Solutions of Coiling Polymers. *J. Chem. Phys.* **1953**, *21*, 1272−1280.
(85) Ferry, J. D. *Viscoelastic Properties of Polymers*; Wiley: New York, 1980.
(86) Bird, R. B.; Curtiss, C. F.; Armstrong, R. C.; Hassager, O. *Dynamics of Polymeric Liquids*; Wiley: 1987; Vol. *2*.
(87) Schweizer, K. S. Microscopic theory of the dynamics of polymeric liquids: General formulation of a mode−mode-coupling approach. *J. Chem. Phys.* **1989**, *91*, 5802−5821.
(88) Farago, J.; Meyer, H.; Baschnagel, J.; Semenov, A. N. Mode-coupling approach to polymer diffusion in an unentangled melt. II. The effect of viscoelastic hydrodynamic interactions. *Phys. Rev. E* **2012**, *85*, 051807.
(89) Farago, J.; Meyer, H.; Semenov, A. N. Anomalous Diffusion of a Polymer Chain in an Unentangled Melt. *Phys. Rev. Lett.* **2011**, *107*, 178301.
(90) Farago, J.; Meyer, H.; Baschnagel, J.; Semenov, A. Hydrodynamic and viscoelastic effects in polymer diffusion. *J. Phys.: Condens. Matter* **2012**, *24*, 284105.
(91) Lowe, C. P.; Masters, A. J. The viscoelastic response of Brownian suspensions. *J. Chem. Phys.* **1999**, *111*, 8708−8720.
(92) Felderhof, B. Cage effect in the viscoelasticity of a suspension of hard spheres without hydrodynamic interaction. *J. Chem. Phys.* **2001**, *114*, 6426−6436.
(93) Saltzman, E. J.; Schweizer, K. S. Large-amplitude jumps and non-Gaussian dynamics in highly concentrated hard sphere fluids. *Phys. Rev. E* **2008**, *77*, 051504.
(94) Cai, C.; Chen, Z. Y. Rouse Dynamics of a Dendrimer Model in the ϑ Condition. *Macromolecules* **1997**, *30*, 5104−5117.

DOI: 10.1021/acs.macromol.7b01058
Macromolecules 2017, 50, 6637−6646

(95) La Ferla, R. Conformations and dynamics of dendrimers and cascade macromolecules. *J. Chem. Phys.* **1997**, *106*, 688−700.
(96) Ganazzoli, F.; La Ferla, R.; Raffaini, G. Intramolecular Dynamics of Dendrimers under Excluded-Volume Conditions. *Macromolecules* **2001**, *34*, 4222−4228.
(97) Gurtovenko, A. A.; Markelov, D. A.; Gotlib, Y. Y.; Blumen, A. Dynamics of dendrimer-based polymer networks. *J. Chem. Phys.* **2003**, *119*, 7579−7590.
(98) Kumar, A.; Biswas, P. Intramolecular relaxation dynamics in semiflexible dendrimers. *J. Chem. Phys.* **2011**, *134*, 214901.
(99) Iwaoka, N.; Takano, H. Relaxation of a Single Dendrimer. *J. Phys. Soc. Jpn.* **2013**, *82*, 064801.
(100) Grimm, J.; Dolgushev, M. Dynamics of internally functionalized dendrimers. *Phys. Chem. Chem. Phys.* **2016**, *18*, 19050−19061.
(101) Yang, Y.; Qiu, F.; Zhang, H.; Yang, Y. The Rouse Dynamic Properties of Dendritic Chains: A Graph Theoretical Method. *Macromolecules* **2017**, *50*, 4007−4021.
(102) Benallal, A.; Marin, G.; Montfort, J. P.; Derail, C. Linear viscoelasticity revisited: the relaxation function of monodisperse polymer melts. *Macromolecules* **1993**, *26*, 7229−7235.
(103) Majeste, J.-C.; Montfort, J.-P.; Allal, A.; Marin, G. Viscoelasticity of low molecular weight polymers and the transition to the entangled regime. *Rheol. Acta* **1998**, *37*, 486−499.
(104) Léonardi, F.; Majesté, J.-C.; Allal, A.; Marin, G. Rheological models based on the double reptation mixing rule: The effects of a polydisperse environment. *J. Rheol.* **2000**, *44*, 675−692.
(105) Liu, C.-Y.; Keunings, R.; Bailly, C. Direct Rheological Evidence of Monomer Density Reequilibration for Entangled Polymer Melts. *Macromolecules* **2007**, *40*, 2946−2954.
(106) Park, S. J.; Desai, P. S.; Chen, X.; Larson, R. G. Universal Relaxation Behavior of Entangled 1,4-Polybutadiene Melts in the Transition Frequency Region. *Macromolecules* **2015**, *48*, 4122−4131.
(107) Fishman, E. Infrared Observation of the O-H Band of Pure Ethanol and Ethanol Solutions to the Critical Temperature. *J. Phys. Chem.* **1961**, *65*, 2204−2208.
(108) Fishman, E.; Li Chen, T. An investigation of the hydrogen bonding characteristics of butanediols. *Spectrochim. Acta, Pt. A: Mol. Spectrosc.* **1969**, *25*, 1231−1242.
(109) Liu, C.; He, J.; Ruymbeke, E. v.; Keunings, R.; Bailly, C. Evaluation of different methods for the determination of the plateau modulus and the entanglement molecular weight. *Polymer* **2006**, *47*, 4461−4479.
(110) Tang, S.; Olsen, B. D. Relaxation Processes in Supramolecular Metallogels Based on Histidine−Nickel Coordination Bonds. *Macromolecules* **2016**, *49*, 9163−9175.
(111) Alexandris, S.; Franczyk, A.; Papamokos, G.; Marciniec, B.; Matyjaszewski, K.; Koynov, K.; Mezger, M.; Floudas, G. Polymethacrylates with Polyhedral Oligomeric Silsesquioxane (POSS) Moieties: Influence of Spacer Length on Packing, Thermodynamics, and Dynamics. *Macromolecules* **2015**, *48*, 3376−3385.
(112) Daniel, W. F. M.; Burdynska, J.; Vatankhah-Varnoosfaderani, M.; Matyjaszewski, K.; Paturej, J.; Rubinstein, M.; Dobrynin, A. V.; Sheiko, S. S. Solvent-free, supersoft and superelastic bottlebrush melts and networks. *Nat. Mater.* **2015**, *15*, 183−189.

DOI: 10.1021/acs.macromol.7b01058
Macromolecules 2017, 50, 6637−6646